Longitudinal pattern of basilar membrane vibration in the sensitive cochlea

Tianying Ren

PNAS 2002;99;17101-17106; originally published online Dec 2, 2002;
doi:10.1073/pnas.262663699

Longitudinal pattern of basilar membrane vibration in the sensitive cochlea

Tianying Ren*

Oregon Hearing Research Center (NRC 04), Department of Otolaryngology and Head and Neck Surgery, Oregon Health and Science University, 3181 Southwest Sam Jackson Park Road, Portland, OR 97239-3098

Communicated by Jozef J. Zwislocki, Syracuse University, Syracuse, NY, November 1, 2002 (received for review September 13, 2002)

In the normal mammalian ear, sound vibrates the eardrum, causing the tiny bones of the middle ear to vibrate, transferring the vibration to the inner ear fluids. The vibration propagates from the base of the cochlea to its apex along the cochlear partition. As essential as this concept is to the theory of hearing, the waveform of cochlear partition vibration has yet to be measured *in vivo*. Here I report a "snapshot" (the instantaneous waveform of cochlear partition vibration) measured in the basal turn of the sensitive gerbil cochlea using a scanning laser interferometer. For 16-kHz tones, the phase delay is up to 6π radians over the observed cochlear length (<1,000 μm), and instantaneous waveforms show sound propagation along the cochlear partition, supporting the existence of the cochlear traveling wave. The detectable basilar membrane response to a low-level 16-kHz tone occurs over a very restricted ($\approx$600 μm) range. The observed vibration shows compressive nonlinear growth, a shorter wavelength, and a slower propagation velocity along the cochlear length than previously reported. Data obtained at different frequencies show the relationship between the longitudinal pattern and frequency tuning, demonstrating that the observed localized traveling wave in this study is indeed the spatial representation of the sharp tuning observed in the frequency domain.

The traveling wave has been considered the fundamental mechanism for analysis of sounds in the cochlea since von Békésy discovered it in human cadavers (1). von Békésy found that the traveling wave amplitude grows linearly with sound intensity (2) and shows a broad peak near the resonant frequency location in the cochlea. To avoid damage caused by invasive procedures, most contemporary *in vivo* studies have measured the vibration at a single location on the basilar membrane (BM). The magnitude and phase of BM vibration velocity or displacement were measured as a function of stimulus frequency, i.e., the magnitude and phase transfer functions. These single-point data from sensitive cochleae have demonstrated compressive nonlinearity and sharp tuning of cochlear vibration in several species (3–16). Our current understanding of cochlear mechanics in sensitive cochleae is based largely on data from single-point measurements. However the spatial pattern of cochlear partition vibration has not yet been described in detail.

To measure the longitudinal pattern of cochlear partition vibration, it is necessary to expose the BM over a wide region and to measure the vibration without placing a reflector on the BM. A large opening in the cochlea very often results in cochlear damage, especially for high frequency hearing. Due to the extremely low reflection coefficient of the cochlear partition (0.0039–0.033%; ref. 17), most measurements using laser interferometry require placement of reflective objects on the cochlear partition. Thus, the measured location is restricted to only the places where beads randomly land. A few technically challenging experiments have been conducted to measure the longitudinal pattern of the BM vibration. Using a laser diode-based feedback interferometer, Russell and Nilsen (13) measured BM vibration without using beads at 11 different positions along the BM in a single guinea pig preparation and at 4 longitudinal locations in another preparation. These authors showed no peak shift of the BM response toward the base with intensity increase and concluded that the site of amplification for the 15-kHz region is restricted to a 1.25-mm length of the BM centered on the 15-kHz location. In chinchilla, Rhode and Recio (18) measured complete transfer functions at eight longitudinal locations on the BM using a heterodyne laser interferometer and reflective beads. Their reconstructed longitudinal pattern of BM vibration based on the transfer functions at different locations showed that, with increasing sound intensity, the location of the maximum BM vibration shifted basally. Later, Nilsen and Russell (19) reported another set of data and showed a peak shift of BM response with intensity increase. However, because of spatial resolution limitations in the above studies, the detailed spatial pattern along the cochlear partition, including the waveform of BM vibration, has not yet been identified. The aim of this study was to measure the magnitude and phase of the transverse velocity of BM vibration and to calculate the instantaneous waveforms, or "snapshots," of the vibration, by using a scanning laser interferometer microscope in the sensitive gerbil cochlea.

Materials and Methods

Thirty young Mongolian gerbils (40–80 g) were used in this study. Animal preparation and surgical approach for opening the bulla were the same as in a previous study (16). The initial anesthesia was induced by i.p. injection of ketamine (30 mg/kg) followed by intramuscular injection of xylazine (5 mg/kg). The animal's head was firmly fixed in a head-holder, which was mounted on a motorized x-y-z translation stage. After a tracheotomy, a ventilation tube was inserted into the trachea to ensure free natural breathing. Rectal temperature was maintained at 38 $\pm$ 1°C with a servo-regulated heating blanket. Animal procedures were approved by the Oregon Health and Science University Institutional Animal Care and Use Committee.

Sensitivity of the ear was monitored by measuring the acoustically induced compound action potential (CAP) through round window and neck electrodes by using the previously described method (16). The CAP was measured several times: immediately after opening an $\approx$3-mm-diameter hole in the bulla, after widely opening the bulla and cutting the middle ear muscles, after removing the round window membrane and surgically enlarging the window, and after completing data collection.

The technique for measurement of BM vibration was developed based on a previous method for beadless single-point measurement of BM vibration (16). Scanning capability was achieved by using a computer-controlled positioning system. Three MFN25CC motorized translation stages (Newport, Irvine, CA) were used to construct a 3D positioning system. With built-in optical position sensors and a closed-loop controller (ESP300, Newport, Irvine, CA), the bidirectional repeatability of the positioning system was <2 μm. LABVIEW-based software was used to automate the controller through a general purpose interface bus (GPIB) interface. A microscope with the sensor

Abbreviations: BM, basilar membrane; CAP, compound action potential; CF, characteristic frequency; SPL, sound pressure level.

*E-mail: rent@ohsu.edu.

head of a modified laser interferometer was mounted on the vertical translation stage. The optical sensitivity of this system was high enough to measure cochlear vibration without the requirement of placing reflective beads on the BM. Therefore, the measurements could be made at any location on the BM.

By removing the round window membrane and then the bony edge to enlarge the opening in the basal and apical directions, ≈1 mm of the BM was exposed. The laser beam from a heterodyne laser interferometer (Polytec CLV, Waldbronn, Germany) was coupled through a custom-built microscope with an infinity-corrected long-working-distance objective (Mitutoyo M Plan Apo ×20, numerical aperture 0.42; Mitutoyo, Kanagawa, Japan) and focused on the BM through a piece of glass coverslip covering the opening. The laser beam reflected from the vibrating BM was collected by the objective and sent back to the laser interferometer. The landmarks of the BM were continuously monitored through a video camera. The voltage output of the interferometer's signal processor was proportional to the transverse vibration velocity. The magnitude and phase of the laser interferometer output was measured by using a lock-in amplifier (SR830 DSP, Stanford Research, Sunnyvale, CA). Acoustic stimulus was generated by a modified dynamic earphone (Sony, Tokyo). The sound source was positioned 1.5 cm from the ear canal opening and calibrated *in situ*. A continuous sinusoidal signal generated by the internal oscillator of the lock-in amplifier was used to drive the earphone. The sound pressure level and the frequency of the tone were controlled by a computer via a programmable attenuator and a GPIB interface.

The focal plane of the laser beam on the BM was determined by the maximum signal level of the interferometer and the sharpest image of the cochlear partition. BM vibration was measured while the laser focus spot was moved from the apical to the basal end of the exposed section of the BM at the rate of 5 μm/s, and a continuous tone at a given frequency and intensity was presented. The scanning path was created by the computer, based on 10–20 reference points approximately along the second row of outer hair cells. The magnitude and the phase of the transverse velocity of BM vibration were collected at the rate of two samples per second, equal to one sample per 2.5 μm in space. Data were collected at different sound pressure levels and frequencies.

Results

Because of the invasive nature of the wide exposure of the BM and the extremely low light intensity reflected from the BM, the productivity of this experiment was very low. A cochlea with an initial CAP threshold at 18 kHz below 15 dB sound pressure level (SPL) and less than 10 dB elevation after data collection was considered a sensitive ear. The normal initial CAP threshold was based on the mean threshold measured from 17 normal animals. Major hearing damage often resulted from enlarging the round window. Hearing sensitivity also deteriorated with time. The data presented below were collected from three of five sensitive cochleae and one insensitive cochlea.

It is possible that opening the cochlea affects its mechanical properties. A mathematical analysis showed that the increased depth of the scala tympani, resulting from the opened round window, could decrease the phase velocity and increase the vibration amplitude (1). However, in this study, the opened round window was covered by using a piece of glass coverslip, and no CAP threshold change after opening the cochlea indicates a relatively physiological cochlear condition. The measurement noise floor in this study is higher, mainly due to the extremely low reflectivity of the BM, than those in experiments using reflective beads, and unavoidable animal movement may have contributed to the results. However, even at the lowest intensity (10 dB SPL), the detected velocity response is >10 dB above the noise floor (≈1 μm/s), and the corresponding phase

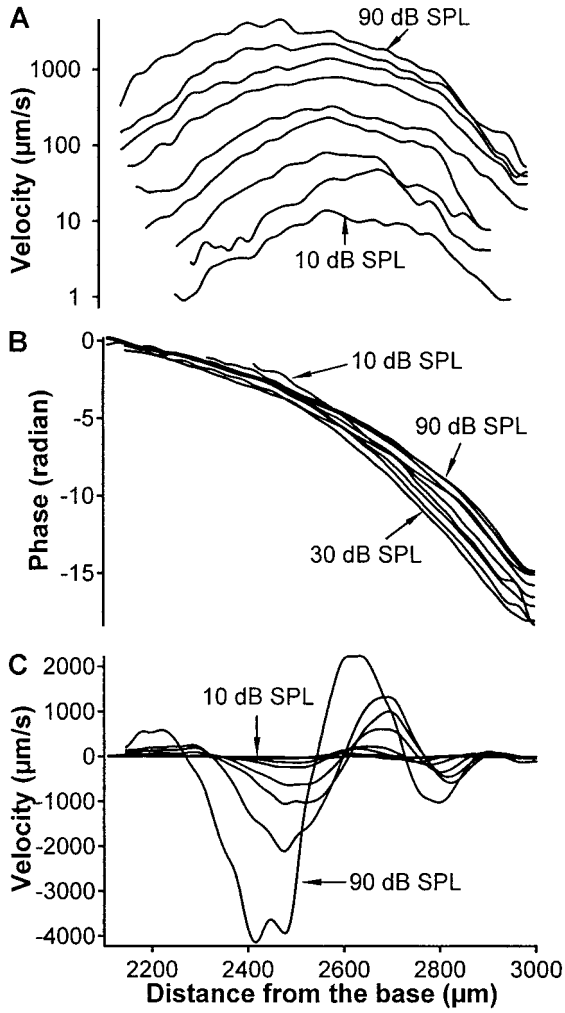

Fig. 1. Transverse velocity magnitude, phase, and instantaneous waveform of BM vibration. Intensity of stimuli is expressed as dB SPL, defined as dB with respect to 20 μPa. The phase is referenced to BM vibration at the basal end of the measured region at 90 dB SPL. (*A*) Magnitude responses to a 16-kHz tone at different intensities are plotted as a function of the longitudinal location. Data show nonlinear compressive growth near and above the CF place, the peak shift toward the base with intensity increase, and the restricted distribution of detectable vibration along the BM at low sound pressure levels. (*B*) Phase curves indicate that, as the wave travels through the range near the CF site, the wavelength becomes shorter and the propagation speed decreases. Phase lag over the observed longitudinal region (<1,000 μm) is as great as ≈6π radians. (*C*) Instantaneous waveforms of BM vibration at different intensities.

showed a similar pattern as those at higher intensities rather than a random change. These features indicate that the data at the low levels were not dominated by the noise.

The magnitudes of the transverse velocities of the BM vibration in response to a 16-kHz tone at different sound pressure levels as a function of longitudinal position are presented in Fig. 1*A* as a typical data set in sensitive cochleae. The initial CAP threshold for this cochlea was 15 dB SPL at 18 kHz before the data collection, and there was less than 5 dB CAP threshold increase during data acquisition. The longitudinal location is indicated by the distance from the basal end of the cochlear partition and measured by using the 3D positioning system along the bony edge of the spiral osseous lamina. The maximal response location, i.e., the characteristic frequency (CF) location, for 16 kHz at 10 dB SPL is ≈2,550 μm from the base. Velocity magnitude at 2,550 μm increased from ≈10 to

≈1,500 μm/s (<45 dB), for a stimulus intensity increase from 10 to 90 dB SPL (80 dB), indicating a nonlinear compression >35 dB. The magnitude–location curves at 10 dB SPL show a broad peak near the 2,550 μm location. The peak broadens more toward the base than toward the apex with intensity increase, especially at higher SPLs, resulting in the peak shifts toward the base. This observation is consistent with the well known peak shift toward the low frequency side with intensity increase shown by magnitude–frequency data (6–16, 20). Magnitude–location curves (Fig. 1*A*) also show that the detectable vibration is confined to a very narrow range along the BM at low SPL. At 10 dB SPL, vibration magnitudes at the basal and apical ends of the observed area fell to the noise floor (≈1 μm/s). Detectable vibratory response to a 10-dB SPL tone occurred over a longitudinal range of ≈600 μm. Thus, Fig. 1*A* shows the nonlinear compressive growth, the peak shift toward the base, and the level-dependent restricted distribution of the vibration along the BM.

Phase as a function of the longitudinal location is presented in Fig. 1*B*. Phase data were collected simultaneously with the magnitude data in Fig. 1*A*, from the same preparation. The phase shows a nonlinear negative relationship with the distance from the base. The flat phase curve near the basal end of the observed location gradually becomes steeper as the vibration propagates toward the apex. Phase lag at the CF for 16 kHz is ≈5 radians and the total phase delay is ≈18 radians over the observed range. Although the phase curves at different intensities almost overlap near the basal end, they are clearly separated near the apical end. At locations apical to the CF site, phase increases with SPL. This intensity-dependent phase change is consistent with single-point measurements of cochlear partition vibration (21, 22) and the data recorded from single auditory nerve fibers (23). In contrast to von Békésy's measurement that the total phase change of the traveling wave in human cadavers is about 3π radians (2), the phase delay in this study is as great as 6π radians over a longitudinal range of <1,000 μm.

The wavelength (λ) and propagation velocity (ν) of BM vibration were calculated according to the following equations: $\nu = \delta x/\delta t = \delta x/[\delta\phi/(2\pi f)]$ and $\lambda = 2\pi\delta x/\delta\phi$, where δt is the travel time over the longitudinal distance δx, $\delta\phi$ is the phase difference between two observed locations in radians, and f is the stimulus frequency in Hz. Phase data indicate that the wavelength and propagation velocity depend on longitudinal location. As the wave propagates through the CF range, the wavelength and propagation velocity decrease dramatically. For a 16-kHz tone, the wavelength and propagation velocity decrease by a factor of twenty over a <1,000-μm observed range. The wavelength and propagation velocity measured at the CF location are ≈200 μm and ≈3.2 m/s. The wavelength and propagation velocity at the locations apical to the CF increase with stimulus intensity.

The waveforms of BM vibration at different sound pressure levels are presented in Fig. 1*C*. The waveforms were constructed based on the real part at each longitudinal location (A_{real}), which was calculated based on the magnitude (A) and the phase (ϕ) according to equation $A_{\text{real}} = A\cos(\phi)$. To show how the wave travels, instantaneous waveforms, or snapshots, of BM vibration at four different times separated by a phase angle of $(1/4)\pi$ radians were calculated (Fig. 2). The vibration envelope (dashed lines) for each sound pressure level was based on data in Fig. 1*A*. A cubic spline function was applied to achieve the smooth waveforms and envelopes in Fig. 2. As the sound pressure increases from 10 to 90 dB SPL, the vibration peaks shift toward the base. The longitudinally compressed waveform at 10 dB SPL spreads out with sound pressure increase, as indicated by the increasingly wider space between the waveforms at higher sound pressure levels. The instantaneous waveforms visually demonstrate the existence of the traveling wave in the living, sensitive cochlea, and present the longitudinal distribution of BM vibration.

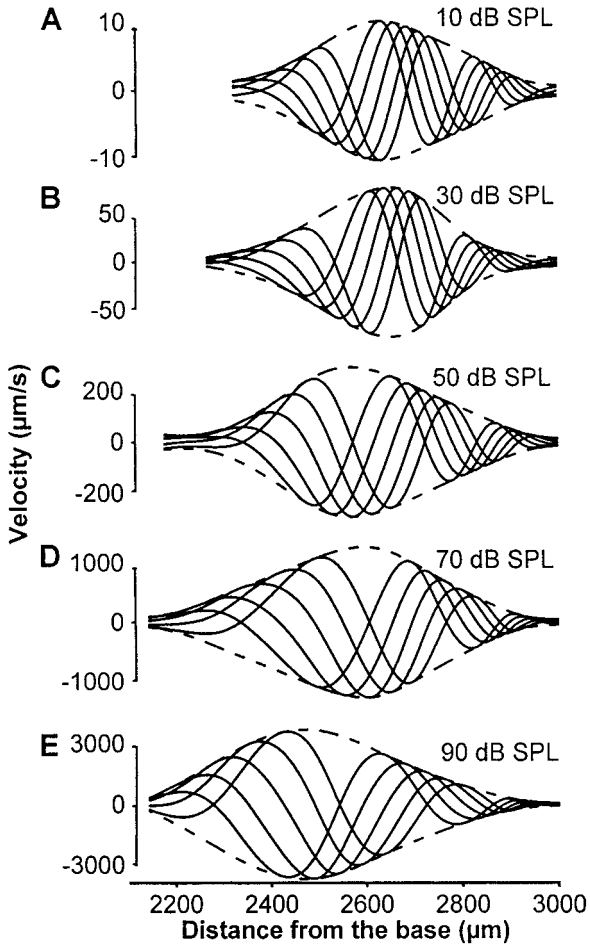

Fig. 2. Time sequences of BM vibrations with sequential $(1/4)\pi$ radians phase intervals at different intensities (10–90 dB SPL). The vibration envelope (dashed lines) for each sound pressure level was obtained by using a cubic spline function based on the data in Fig. 1*A*. Solid lines are instantaneous waveforms. Vibration peaks shift toward the base, and the longitudinally compressed waveforms spread out with sound pressure increase.

Fig. 3 compares the longitudinal pattern of BM responses in sensitive with that in insensitive cochleae. Insensitive data were collected from a postmortem cochlea ≈10 min after death. Postmortem data were collected by using 16-kHz tones at 60 and 70 dB SPL. Sensitive data are from Fig. 1*A* at the same sound intensities. Near the 16-kHz CF location (≈2,550 μm), the velocity in the insensitive cochlea is >30 dB less than in the sensitive cochlea. Although the solid lines show broad peaks, indicating maximum BM response inside the observed section of the BM, the dashed lines show no peak over the same region. The fact that the maximum response is located at the basal end of the observed region implies that the peak response in the insensitive cochlea probably was at the location basal to the observed region. Unequal narrowly spaced two solid lines indicate that, for a 10-dB increase of sound intensity from 60 to 70 dB SPL, the transverse velocity of BM vibration of the sensitive cochlea showed longitudinal location-dependent and less than 10-dB increase, demonstrating the location-dependent compressive growth. In contrast to the solid lines, the two dashed lines are approximately parallel and with ≈10 dB separation, indicating a linear BM response in the insensitive cochlea. The flatter overall phase slope and much smaller phase lag of the dashed lines than

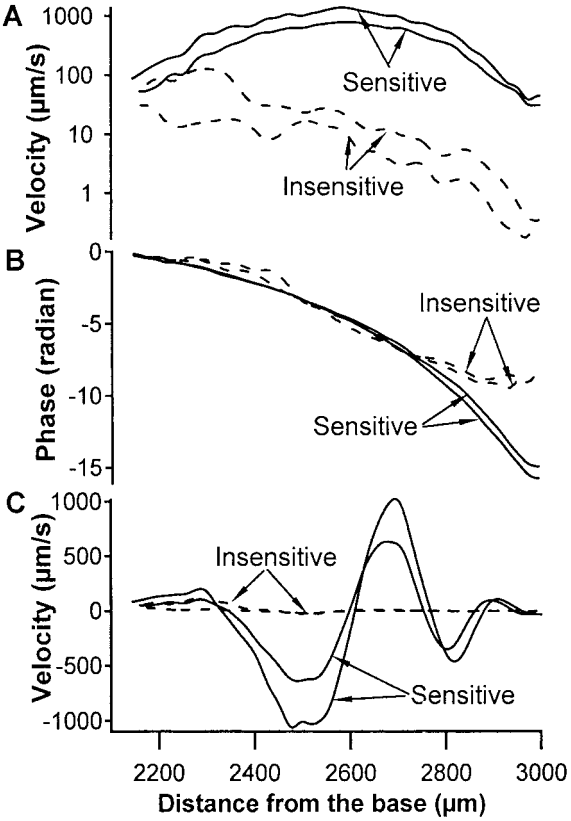

Fig. 3. Longitudinal patterns of the magnitude and phase of the transverse velocity of BM responses in sensitive and insensitive cochleae. Insensitive data were collected by using 16-kHz tones at 60 and 70 dB SPL ≈10 min postmortem, and sensitive data are from Fig. 1*A*. Near the 16-kHz CF location (≈2,550 μm), the velocity in the insensitive cochlea is >30 dB less than in the sensitive cochlea. The overall peak in the sensitive cochlea (solid lines) disappeared in the insensitive cochlea (dashed lines). The wider separation between the two dashed lines than between the solid lines indicates linear growth in the postmortem cochlea. (*B*) The flatter overall phase slope and the much smaller phase lag of the dashed lines than the solid lines represent a longer wavelength and a faster propagation velocity in the insensitive cochlea. (*C*) The instantaneous waveforms.

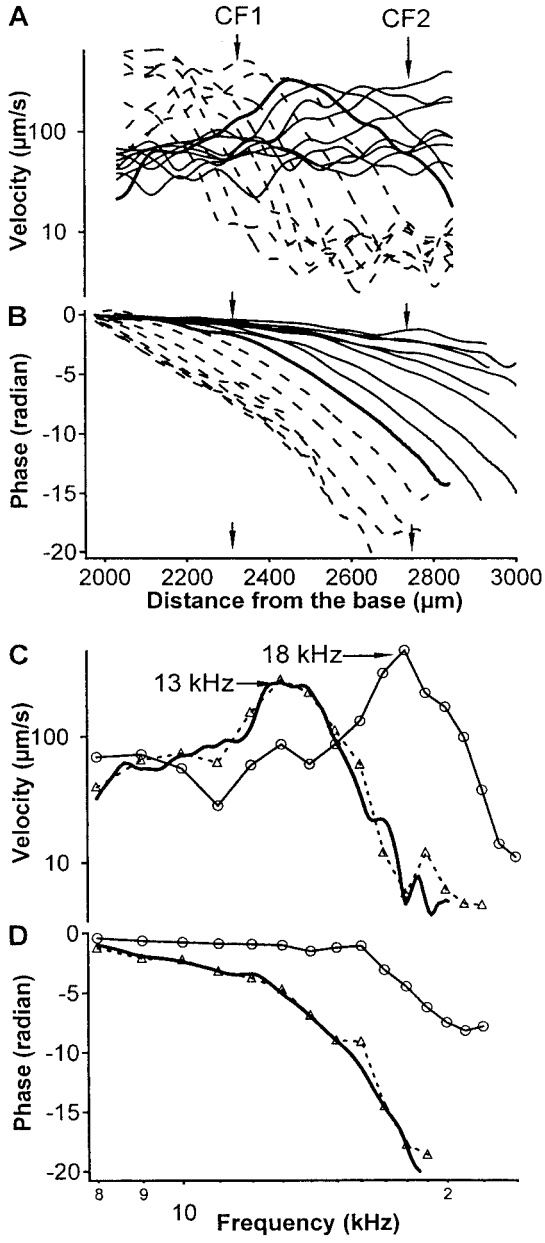

Fig. 4. The relationship between the longitudinal pattern and the frequency tuning of BM vibration. (*A*) The longitudinal patterns of BM responses to tones at different frequencies from 8 to 24 KHz in 1-kHz steps and at a constant intensity of 60 dB SPL. The thick solid line is 16 kHz, dashed lines are frequencies >16 kHz, and thin solid lines are frequencies <16 kHz. (*B*) Phase curves. (*C* and *D*) Magnitude and phase transfer functions. Magnitude transfer function based on data at ≈2,750 μm (dashed line) shows a response peak at ≈13 kHz, and magnitude transfer function based on data at ≈2,300 μm (thin solid line) shows a peak at ≈18 kHz. Thick solid lines in *C* and *D* are the magnitude and phase transfer functions measured in another sensitive cochlea at 60 dB SPL, which closely match dashed lines.

the solid lines in Fig. 3*B* represent a longer wavelength and faster propagation velocity in the insensitive cochlea. Waveform is much smaller in the insensitive cochlea in Fig. 3*C*, confirming the postmortem changes shown in Fig. 3*A*.

The longitudinal pattern of BM transverse velocity in response to tones at different frequencies is presented in Fig. 4*A*. Tones between 8 and 24 kHz in 1-kHz steps and at a constant intensity of 60 dB SPL were presented to the same sensitive ear; the transverse velocity magnitude and phase of BM vibration were measured as functions of the longitudinal location. Data points of the transverse velocity near the basal and apical ends were removed to eliminate the potential effect of noise caused by the low reflected light near the edges of the cochlear opening. The peak location of the BM response is a function of the stimulus frequency. The peak location for a high frequency tone is near the basal end of the observed area, and the peak response shifts toward the apex as the stimulus frequency decreases. The sharpness of the BM response peak is closely related to the stimulus frequency: BM response to a high frequency tone shows a sharper peak than for a low frequency tone. The longitudinal phase patterns of BM responses to tones at different frequencies are presented in Fig. 4*B*. Although the overall pattern of the phase curves is similar across frequencies, the slope of the phase curves decreases with increasing frequency, i.e., at any given location, the phase lag increases with frequency increase.

To show the relationship between the spatial pattern and the frequency tuning of BM vibration, all magnitude and phase data points at the ≈2,300- and ≈2,750-μm locations were plotted as functions of frequency in Fig. 4 *C* and *D*. The magnitude–frequency curve based on data at ≈2,750 μm shows a response peak at ≈13 kHz, and that from location ≈2,300 μm a peak at

≈18 kHz. Thick solid lines in Fig. 4 *C* and *D* present magnitude and phase transfer functions of the transverse velocity of the BM vibration measured in another sensitive cochlea at 60 dB SPL. The data were collected as a function of the frequency from the single point on the BM at a longitudinal location of ≈2,700 μm. Thick solid lines in Fig. 4 *C* and *D* closely match the shape of the dashed lines, indicating that the frequency responses derived from the spatial pattern are consistent with transfer functions measured at a single point on the BM. Data in Fig. 4 also show that an ≈450-μm change in longitudinal location resulted in approximately a 5-kHz change in the frequency of maximum response.

Discussion

Distribution of Transverse Vibration Along the Cochlear Partition. By observing BM vibration at low frequency and high intensity in human cadavers, von Békésy found that, although the amplitudes fell off relatively sharply on the side toward the helicotrema, the vibration extended toward the base and down to the stapes (2). Based on this observation, it has been widely believed that cochlear vibration starts at the base and propagates along the cochlear partition. Data presented in Fig. 1*A* show that the longitudinal extent of the BM response to a 16-kHz tone *in vivo* is intensity-dependent. For low-level tones below 30 dB SPL, the longitudinal pattern of detectable BM vibration is restricted to a region of ≈600 μm. Data in Fig. 4*A* indicate that the longitudinal pattern is also frequency-dependent. As the frequency decreases, in addition to the shift of the BM vibration peak toward the apex, the longitudinal extent increases significantly.

As sound levels increase, the detectable BM excitation pattern extends toward the base and apex, and the peak BM response shifts toward the base. Due to the limited length of the observed region in this study, the complete spatial pattern of BM responses to high-level tones could not be shown. However, the patterns of the magnitude curves in Figs. 1 and 3 indicate that the response peak, spread with sound-level increase, is greater toward the base than toward the apex. The curves diverge in the former direction and converge in the latter, especially for higher SPLs. This asymmetry is consistent with the classical cochlear traveling wave. Although there are inconsistent reports on the existence of the peak shift toward the base with sound-level increase (13, 18, 19), all sensitive gerbil cochleae in this study showed this basal shift with sound-level increase. The extent of this maximum response peak shift is closely related to cochlear sensitivity; i.e., the more sensitive cochleae showed greater shift toward the base, which is consistent with the peak shift to low frequencies (24).

Phase as a Function of Longitudinal Location. von Békésy (2) found that the amplitude spatial pattern alone could not distinguish a pure resonant system from a traveling wave. His concept of the cochlear traveling wave was based mainly on phase data, because a pure resonant system cannot result in the 3π radians phase change he observed (25). In this study, the phase of the transverse velocity of cochlear partition vibration was measured in great detail as a function of longitudinal location in sensitive gerbil cochlea. The data in Figs. 1*B* and 4*B* show that, as the vibration propagates through the observed area (<1,000 μm), the phase changes up to $\approx 6\pi$ radians for the 16-kHz CF tone. Thus, the vibration observed in this study supports the existence of the traveling wave *in vivo*. The fine spatial resolution of measurement used in this study made it possible to calculate instantaneous waveforms, or snapshots, of BM vibration, based on the magnitude and phase of the transverse velocity measured from different longitudinal locations. Fig. 2 visually presents the cochlear partition vibration in time and space.

Although the mean wavelength and propagation velocity from the base to the CF location can be calculated based on the phase transfer function measured at a single location on the BM, it provides no information on the wavelength and propagation velocity as a function of the longitudinal location. Figs. 1*B* and 4*B* unambiguously show that the slope of the phase curves, indicating the wavelength and propagation velocity, depends on longitudinal location, stimulus frequency, and sound intensity.

Based on the phase data in Fig. 1*B*, the wavelength and propagation velocity at the 16-kHz CF location are ≈200 μm and ≈3.2 m/s, respectively, which are significantly shorter and slower than those reported in the literature (4, 11, 18, 26, 27). In his pioneering work, Rhode (4) measured amplitude and phase as a function of the stimulus frequency at two different locations, ≈1.5 mm apart, on the BM in the squirrel-monkey cochlea. He found that the propagation velocity of BM vibration is about 12 m/s for low frequencies and decreases to about 9 m/s as the maximally effective frequency is approached. Cooper and Rhode (11) found the wavelength at the 31-kHz CF location to be 0.6 mm in the cat and 0.9 mm in the guinea pig. Olson (26, 27) showed a traveling-wave wavelength just below 1 mm for a 23-kHz tone, estimated from the phase data of the intracochlear pressure measured at two locations separated by 1.8 mm in the basal turn of the gerbil cochlea. By measuring cochlear partition vibration from multiple beads on the BM along the cochlear length in the basal region of the chinchilla cochlea, Rhode and Recio (18) found that, for frequencies below the CF, the traveling wave velocity could be as high as 100 m/s but the velocity was only ≈8 m/s at the CF. The wavelength of cochlear partition vibration in different animals has been reviewed recently by Robles and Ruggero (28). Although animal species, stimulus frequency and level, and BM location all contribute to the measured results of wavelength and propagation velocity, the inconsistency between results in this study and those in the literature is probably partially methodological. Due to the dispersive feature of the cochlear partition, the wavelength and propagation velocity vary with longitudinal location, as indicated by the location-dependent phase slope in Figs. 1*B* and 4*B*. For measuring wavelength and propagation velocity at a particular location on the BM, a spatial resolution much smaller than the wavelength is needed. The spatial resolution used in the literature is determined by the separation of two measured points, which are significantly longer than the wavelength to be measured. Thus, the wavelengths reported in the literature are averaged over the distance between two measured points, whereas the wavelength and propagation velocity measured in this study are location specific. The wavelength at CF can be expected to be even smaller than 200 μm according to a model prediction (1).

Longitudinal Pattern and Sharp Tuning. In sensitive cochleae, the cochlear partition vibration at a given location shows a maximum response to a stimulus at the CF, falls off quickly at frequencies above or below the CF, and forms a sharp peak in magnitude transfer functions. Sharp tuning has been well documented based on single-point vibration measurements on the BM (29). To show the relationship between the longitudinal pattern and the frequency tuning of BM vibration, vibration measured as a function of the longitudinal location at different frequencies (Fig. 4 *A* and *B*) was presented as a function of the frequency at two given locations (Fig. 4 *C* and *D*). The frequency responses derived from the longitudinal pattern are consistent with transfer functions measured from a single point on the BM (thick solid lines in Fig. 4 *C* and *D*), demonstrating that the localized BM vibration along the longitudinal direction is the spatial representation of the sharp

tuning. To understand how the cochlea achieves high sensitivity, sharp tuning, and nonlinearity, an outer hair cell-based feedback mechanism, or cochlear amplifier, has been proposed to provide electromechanical amplification of the traveling wave (1, 30). Considering that the restricted longitudinal extent of BM vibration is the spatial representation of the sharp tuning, the question of how spatially restricted vibration occurs in the sensitive cochlea seems to be as important as how the cochlea achieves the sharp tuning. These new quantitative data on the longitudinal pattern of BM vibration will provide valuable information to explore such questions.

I thank A. L. Nuttall for valuable discussions, S. Matthews and E. Porsov for technical support, Y. Zou for assistance in data collection and processing, and P. Gillespie, F. Zeng, and E. De Boer for comments on early drafts of the manuscript. This work was supported by the National Institute of Deafness and Other Communication Disorders and the National Center for Rehabilitative Auditory Research, Portland Veterans Affairs Medical Center.

1. Zwislocki, J. J. (2002) *Auditory Sound Transmission: An Autobiographical Perspective* (Lawrence Erlbaum, Mahwah, NJ).
2. von Békésy, G. (1960) *Experiments in Hearing* (McGraw–Hill, New York).
3. Khanna, S. M. & Leonard, D. G. (1982) *Science* **215,** 305–306.
4. Rhode, W. S. (1971) *J. Acoust. Soc. Am.* **49,** 1218–1231.
5. Sellick, P. M., Patuzzi, R. & Johnstone, B. M. (1982) *J. Acoust. Soc. Am.* **72,** 131–141.
6. Robles, L., Ruggero, M. A. & Rich, N. C. (1986) *J. Acoust. Soc. Am.* **80,** 1364–1374.
7. Ruggero, M. A., Robles, L. & Rich, N. C. (1986) *J. Acoust. Soc. Am.* **80,** 1375–1383.
8. Ruggero, M. A., Robles, L., Rich, N. C. & Recio, A. (1992) *Philos. Trans. R. Soc. London B Biol. Sci.* **336,** 307–314.
9. Nuttall, A. L., Dolan, D. F. & Avinash, G. (1991) *Hear. Res.* **51,** 203–213.
10. Ruggero, M. A. & Rich, N. C. (1991) *Hear. Res.* **51,** 215–230.
11. Cooper, N. P. & Rhode, W. S. (1992) *Hear. Res.* **63,** 163–190.
12. Nuttall, A. L. & Dolan, D. F. (1996) *J. Acoust. Soc. Am.* **99,** 1556–1565.
13. Russell, I. J. & Nilsen, K. E. (1997) *Proc. Natl. Acad. Sci. USA* **94,** 2660–2664.
14. Murugasu, E. & Russell, I. J. (1996) *J. Neurosci.* **16,** 325–332.
15. Khanna, S. M. & Hao, L. F. (2000) *Hear. Res.* **149,** 55–76.
16. Ren, T. & Nuttall, A. L. (2001) *Hear. Res.* **151,** 48–60.
17. Khanna, S. M., Willemin, J. F. & Ulfendahl, M. (1989) *Acta Otolaryngol. Suppl.* **467,** 69–75.
18. Rhode, W. S. & Recio, A. (2000) *J. Acoust. Soc. Am.* **107,** 3317–3332.
19. Nilsen, K. E. & Russell, I. J. (2000) *Proc. Natl. Acad. Sci. USA* **97,** 11751–11758.
20. Chatterjee, M. & Zwislocki, J. J. (1997) *Hear. Res.* **111,** 65–75.
21. Ruggero, M. A., Rich, N. C., Recio, A., Narayan, S. S. & Robles, L. (1997) *J. Acoust. Soc. Am.* **101,** 2151–2163.
22. Nuttall, A. L. & Dolan, D. F. (1993) *J. Acoust. Soc. Am.* **93,** 390–400.
23. Anderson, D. J., Rose, J. E., Hind, J. E. & Brugge, J. F. (1971) *J. Acoust. Soc. Am.* **49,** 1131–1139.
24. Zhang, M. & Zwislocki, J. J. (1996) *Hear. Res.* **96,** 46–58.
25. Zwislocki, J. J. (1974) *J. Acoust. Soc. Am.* **55,** 578–583.
26. Olson, E. S. (1998) *J. Acoust. Soc. Am.* **103,** 3445–3463.
27. Olson, E. S. (1999) *Nature* **402,** 526–529.
28. Robles, L. & Ruggero, M. A. (2001) *Physiol. Rev.* **81,** 1305–1352.
29. Narayan, S. S., Temchin, A. N., Recio, A. & Ruggero, M. A. (1998) *Science* **282,** 1882–1884.
30. Dallos, P. (1992) *J. Neurosci.* **12,** 4575–4585.